

Available online at www.sciencedirect.com

ScienceDirect

www.elsevier.com/locate/jmbbm

Research Paper

Failure modes of Y-TZP abutments with external hex implant-abutment connection determined by fractographic analysis

Mariana de Almeida Basílio^{a,*}, Juliana Aparecida Delben^a,
Paulo Francisco Cesar^b, Amin Sami Rizkalla^c, Gildo Coelho Santos Junior^d,
João Neudenir Arioli Filho^a

^aUNESP – University Estadual Paulista, Araraquara School of Dentistry, Department of Dental Materials and Prosthodontics, 1680, Araraquara 14801-903, SP, Brazil

^bUSP – University of São Paulo, School of Dentistry, Department of Biomaterials and Oral Biology, 2227, São Paulo 05508-000, SP, Brazil

^cWestern University, Schulich School of Medicine & Dentistry, Department of Medical Biophysics, Medical Sciences Building, London, ON, Canada N6A 5C1

^dWestern University, Schulich School of Medicine & Dentistry, Department of Dentistry, Medical Sciences Building, London, ON, Canada N6A 5C1

ARTICLE INFO

Article history:

Received 10 June 2015

Received in revised form

19 December 2015

Accepted 25 December 2015

Available online 6 January 2016

Keywords:

Fractography

Failure analysis

Implant abutment

Zirconia

Dental ceramic

ABSTRACT

Yttria-stabilized tetragonal zirconia (Y-TZP) was introduced as ceramic implant abutments due to its excellent mechanical properties. However, the damage patterns for Y-TZP abutments are limited in the literature. Fractographic analyses can provide insights as to the failure origin and related mechanisms. The purpose of this study was to analyze fractured Y-TZP abutments to establish fractographic patterns and then possible reasons for failure. Thirty two prefabricated Y-TZP abutments on external hex implants were retrieved from a single-load-to failure test according to the ISO 14801. Fractographic analyses were conducted under polarized-light estereo and scanning electro microscopy. The predominant fracture pattern was abutment fracture at the connecting region. Classic fractographic features such as *arrest lines*, *hackle*, and *twist hackle* established that failure started where Y-TZP abutments were in contact with the retention screw edges. The abutment screw design and the loading point were the reasons for localized stress concentration and fracture patterns.

© 2016 Elsevier Ltd. All rights reserved.

*Corresponding author.

E-mail addresses: mariana_basilio@yahoo.com.br (M.d.A. Basílio), ju.delben@hotmail.com (J.A. Delben), paulofc@usp.br (P.F. Cesar), arizkalla@eng.uwo.ca (A.S. Rizkalla), gildo.santos@schulich.uwo.ca (G.C. Santos Junior), arioli@foar.unesp.br (J.N. Arioli Filho).<http://dx.doi.org/10.1016/j.jmbbm.2015.12.042>

1751-6161/© 2016 Elsevier Ltd. All rights reserved.

1. Introduction

The use of yttria-stabilized tetragonal zirconia (Y-TZP) has extended the application of all-ceramic restorations to a great number of clinical situations, including all-ceramic abutments in which strength and esthetics in the gingival area are critical.

Clinical studies evaluating Y-TZP abutments reported promising results for an observational period of three to four years in which the abutments provided appropriate stability for single-tooth implant restorations and resisted fracture (Glauer et al., 2004; Zembic et al., 2009). Y-TZP abutments showed outcomes similar to titanium abutments in posterior regions as both exhibited 100% survival rates in two clinical studies (Lops et al., 2013; Zembic et al., 2009). A prospective clinical study on Y-TZP abutments supporting single-tooth crowns exhibited excellent long-term outcomes with a cumulative success rate of 96.3% after 11 years of use (Zembic et al., 2015). However, clinical reports of catastrophic failures do exist (Aboushelib and Salameh, 2009; Passos et al., 2014) and, thus, such predictions must be moderated by the relatively short-term evaluation in most prospective studies. Indeed, the aforementioned clinical studies did not fully explain the reasons why restoration fracture occurs.

Currently, the damage patterns are assessed from retrieved structures that fractured in clinical use by means of fractography. However, the information regarding Y-TZP abutments is limited by the number of studies and abutments analyzed. In this sense, a systematic fractographic analysis may provide relevant information about crack initiation sites, fracture paths, stress accumulation and then possible reasons for failure. In 2013, *çilo et al. (2013)* stated that when a laboratory study adequately mimics the clinical fracture resistance and the clinical fracture features, it

represents an in vitro design with high clinical significance. Thus, evaluating the failure mode of Y-TZP abutments according to the ISO 14801 (ISO 14801:2007) appears to be useful, since the test procedure recommended by this standard simulates the functional loading of an endosseous dental implant and its prosthetic components under the worst in vivo scenario.

The purpose of this study was to use fractographic principles to analyze the broken parts of Y-TZP abutments tested in vitro, revealing discriminatory landmarks that would help to establish fracture patterns and then possible reasons for failure. In addition, the findings would support further fractographic analyses of retrieved Y-TZP implant restorations.

2. Materials and methods

Thirty two prefabricated Y-TZP abutments (Neodent-Implante Osteointegrável Curitiba, PR, Brazil) were screwed and torqued down to external hex implants and divided into 4 groups ($n=8$), according to the ageing condition: 1 – no further treatment (control), 2 – mechanical aging in water (1×10^6 cycles, 10 Hz, at 37 °C), 3 – accelerated aging for 5 h in autoclave (134 °C, 2 bars), 4 – thermal cycling (1×10^4 cycles, between 5° and 55 °C). After ageing, all groups were subjected to a single-load-to-fracture test using a 30° angled steel holder in a universal testing machine MTS 801 (Material Test System, Edem Prairie, MN, USA). A metallic hemispherical cap was temporarily cemented (Provy; Dentsply, Catanduva, SP, Brazil) on every Y-TZP abutment, ensuring that the loading center was at a longitudinal distance of 11 mm from the support level of the implant (ISO 14801:2007). The load-to-fracture test was carried out at a crosshead speed of 0.5 mm/min until the failure.

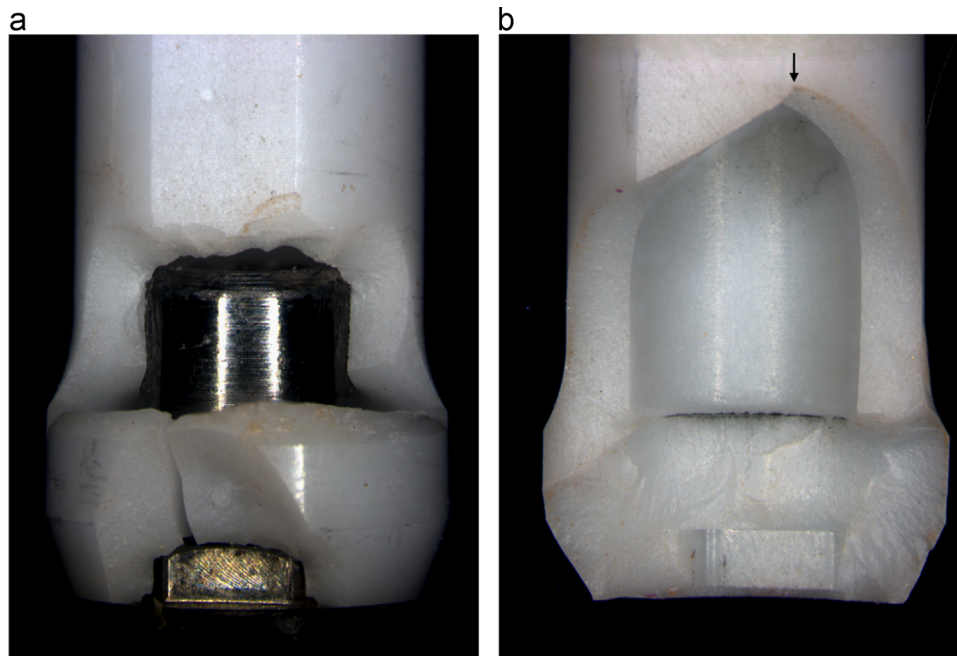


Fig. 1 – (a) Stereomicroscopic image of an abutment showing multiple fractures at the connecting region. (b) Stereomicroscopic image of an abutment showing the fracture near the loading area (small black arrow).

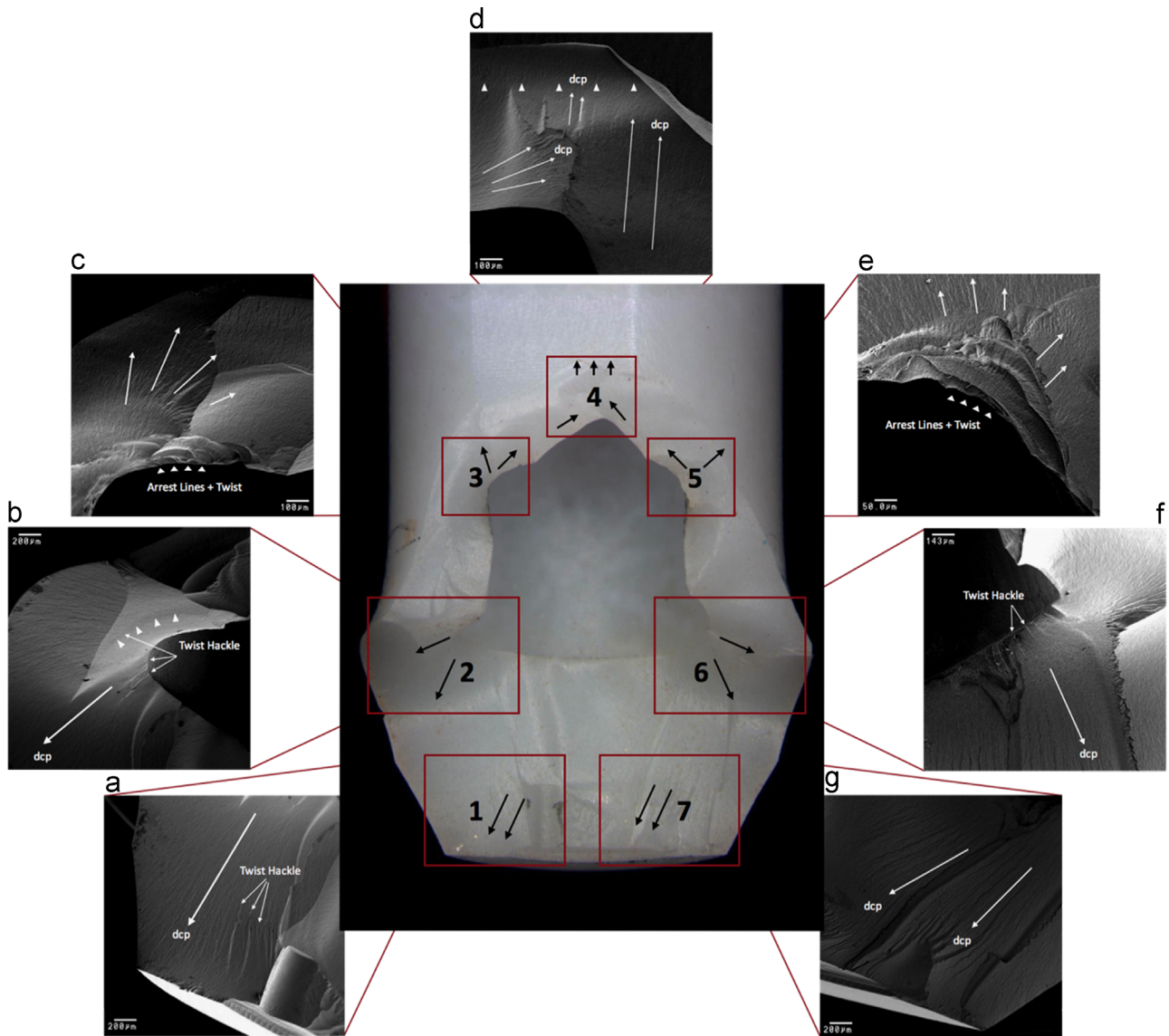


Fig. 2 – Representative abutment exposing part of the fracture surface examined under the SEM. Zones of interest are numbered 1–7 starting at the left margin to the other side of the abutment. Black arrows have been drawn indicating the general directions of crack propagation.

After analyzing the macroscopic aspects of the fracture patterns, the fracture surfaces of the abutments were inspected under polarized microscopy (SteREO Discovery V20, Zeiss, Germany). The stereomicroscope analysis was performed at low magnification in order to obtain an overview of the specimen topography and detection of crack features. The representative failed abutments were gold sputtered (Leica EM SCD-500, Leica Mikrosysteme GmbH, Vienna, Austria) and further observed using a scanning electron microscope (SEM) (Model SM-300, Topcon Corporation, Tokyo, Japan) at high magnification.

In addition, the fracture surface examination of the most representative abutments was performed in selected areas of interest following the systematic approach proposed by Scherrer et al. (2008) to create an overall view of the failed components and then suggest possible reasons for failure (Figs. 2–5).

3. Results

There were no differences in fracture patterns and fractographic features among the control and aged groups.

The initial stereo analysis revealed that two fracture patterns could be identified. The predominant scenario observed in all groups was abutment fracture at the connecting region originated from the abutment screw head and hexagon vertex (Fig. 1a). However, some specimens also showed abutment fracture near the loading area which suggested that the failure originated from the loading point and then propagated downwards (Fig. 1b).

Fig. 2 shows a representative abutment of the fracture pattern near the loading area and the zones of interest for detailed fractographic analysis according to the systematic approach proposed by Scherrer et al. (2008). The analysis started at the left gingival margin of the fracture surface,

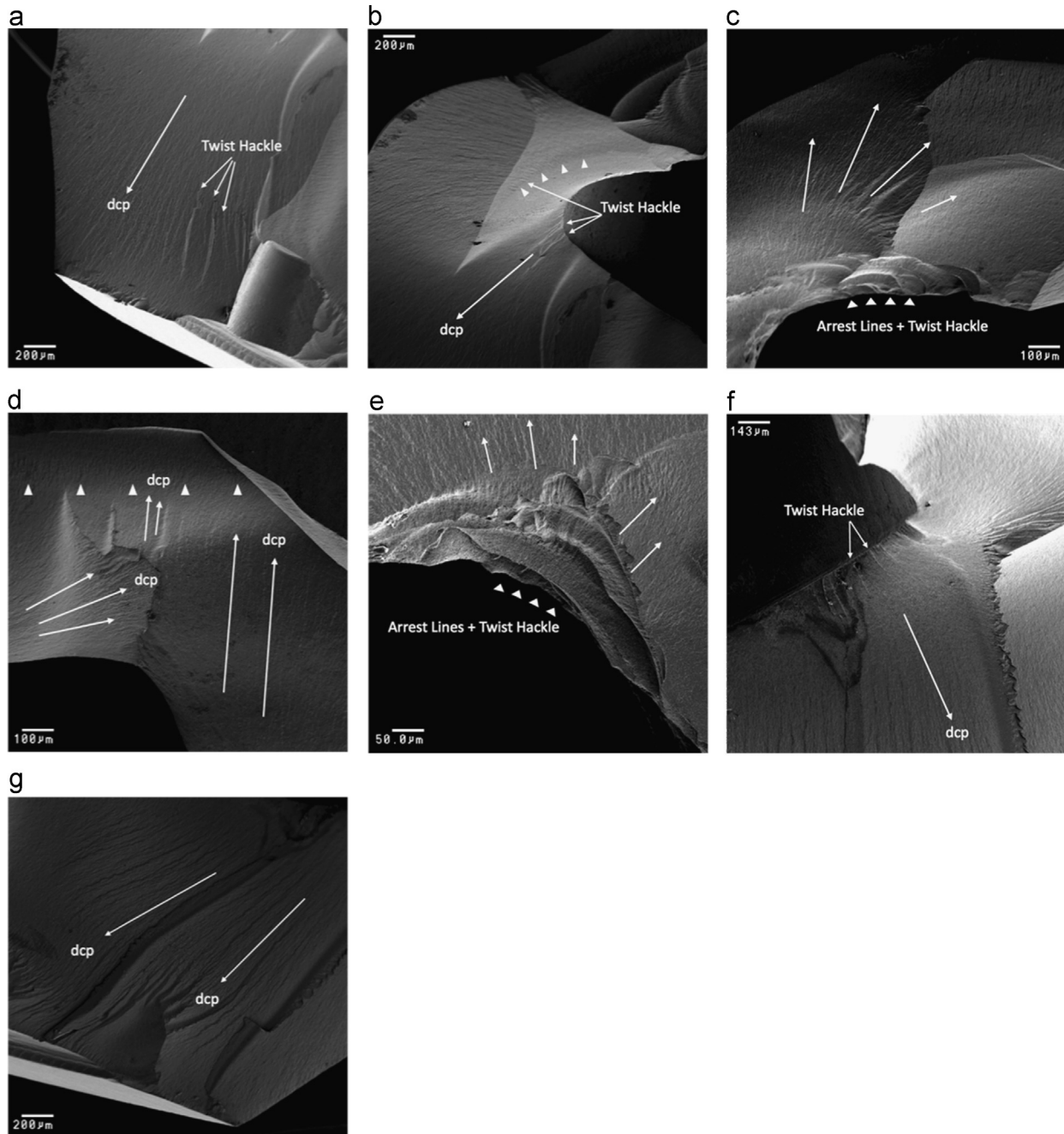


Fig. 3 – (a) SEM image of zone 1. Fractographic features like *twist hackle* are clearly visible on the fracture surface as indicated by the arrows. Indeed, many micro-fine texture *hackle lines* are propagating downwards to the gingival margin of the abutment. These features provide clear indication as to the direction of crack propagation (*dcp*) in this region (big white arrow). **(b)** SEM image of zone 2 showing *twist hackle* emanating from the abutment region that was in contact with the lower edge of the abutment screw head and these fine *hackle* together with a lateral arrest line (white arrowheads). These fractographic features confirmed that the fracture front moved from this region towards the gingival area and laterally. Other features are visible in Fig. 3b and serve as an evidence of *dcp* like micro-fine *hackle lines*. **(c)** SEM image of zone 3 showing multiple origins (damages) in the form of radial *arrest lines*. It is also possible to note the presence of *twist hackle lines* departing from the damage zone and connecting adjacent *arrest lines* (white arrowheads). Arrays of *hackle* moving laterally and upwards could also be identified (white arrows). **(d)** SEM image of zone 4 showing multiple micro-fine *hackle* propagating to the occlusal area as a result of the crack path moving from both proximal sides. Indeed, the existence of a *compression curl*, which is the curved lip just before the total fracture of a body loaded in bending, confirmed that the crack moved outwards exiting at the occlusal wall (white arrowheads in Fig. 4d). **(e)** SEM image of zone 5 showing fractographic features (radially *arrest lines* from which *twist hackle* emanated) like the homologous zone. **(f)** SEM image of zone 6 showing fractographic features (*twist hackle* and micro-fine *hackle lines*) like the homologous zone. **(g)** SEM image of zone 7 showing fractographic features (micro-fine *hackle lines*) like the homologous zone.

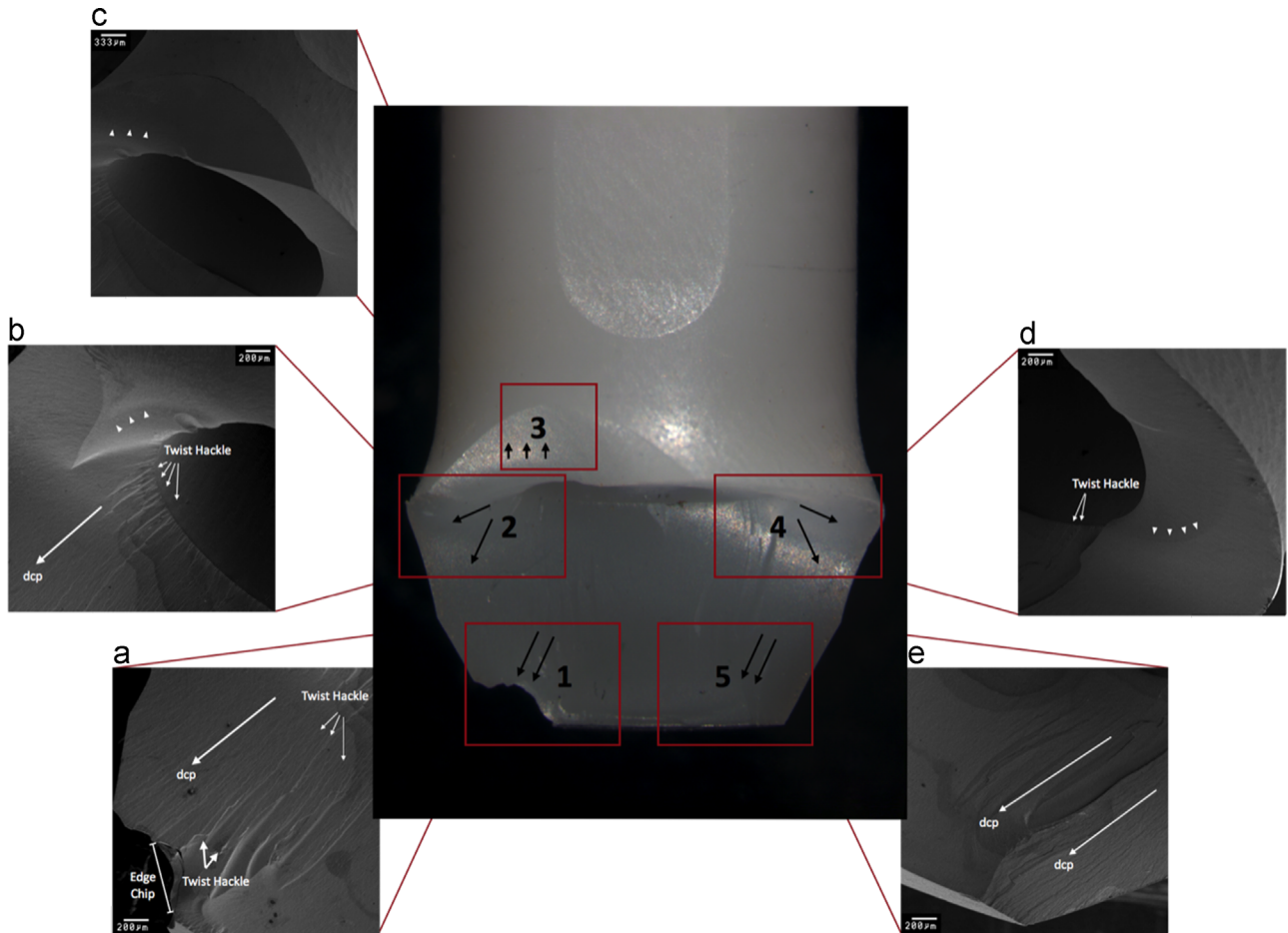


Fig. 4 – Representative abutment exposing part of the fracture surface examined under the SEM. Zones of interest are numbered 1–5 starting at the left margin to the other side of the abutment. Black arrows have been drawn indicating the general directions of crack propagation.

moving upwards towards the occlusal section and finishing at the right end side of the abutment (numbers 1–7 in Fig. 2). Based on the microscope findings, a final map was then created on the overall view of the representative abutment indicating the general directions of crack propagation.

The initial SEM inspection of zone 1 (Fig. 3a) indicated that the crack was running downwards. The big white arrow labeled “dcp” shows the direction of the crack propagation. The SEM image of zone 2 (Fig. 3b), which corresponds to the abutment region that was in contact with the lower edge of the abutment screw head, indicated that the dcp moved from this region downwards and laterally. The inspection of zone 3 (Fig. 3c), which corresponds to the abutment region that was in contact with the upper edge of the abutment screw head, exhibited one area of multiple origins based on radially arrest lines from which twist hackle emanated. It was possible to observe the crack propagation from both proximal sides under the SEM analysis of zone 4 (Fig. 3d). The large arrows indicate the dcp. Furthermore, zones on the right side exhibited fractographic features like those of the homologous zones on the left side (Fig. 3e–g).

Fig. 4 shows a representative abutment of the fracture pattern related to the connecting region and the zones of interest for detailed fractographic analysis (Scherrer et al.,

2008). Based on the microscope findings, a final map was then created on the overall view of the representative abutment indicating the general directions of crack propagation.

The SEM image of zone 1 (Fig. 5a) showed twist hackle and many micro-fine hackle lines propagating downwards as well as in the corresponding zone of the above-described abutment. The SEM image of zone 2 (Fig. 5b) revealed exactly the same landmarks as those observed in the corresponding zone of the above-described abutment. These fractographic features confirmed that the fracture front originated from this region and therefore, the abutment screw directly affected the occurrence of failure. Indeed, the inspection of zone 3 (Fig. 5c) showed a compression curl which confirmed that the crack moved outwards exiting at the occlusal wall. The zones on the right side exhibited fractographic features like those of the homologous zones on the left side (Fig. 5d and e).

Fig. 6 shows two arrest lines visible on a broken part from the connecting region of another representative abutment providing evidence that damage started at this region. The failure origin is located on the concave side of the first arrest line, i.e., near the edge of the abutment screw head. A close-up image of Fig. 6 under the SEM confirmed the presence of these features including hackle lines (Fig. 7).

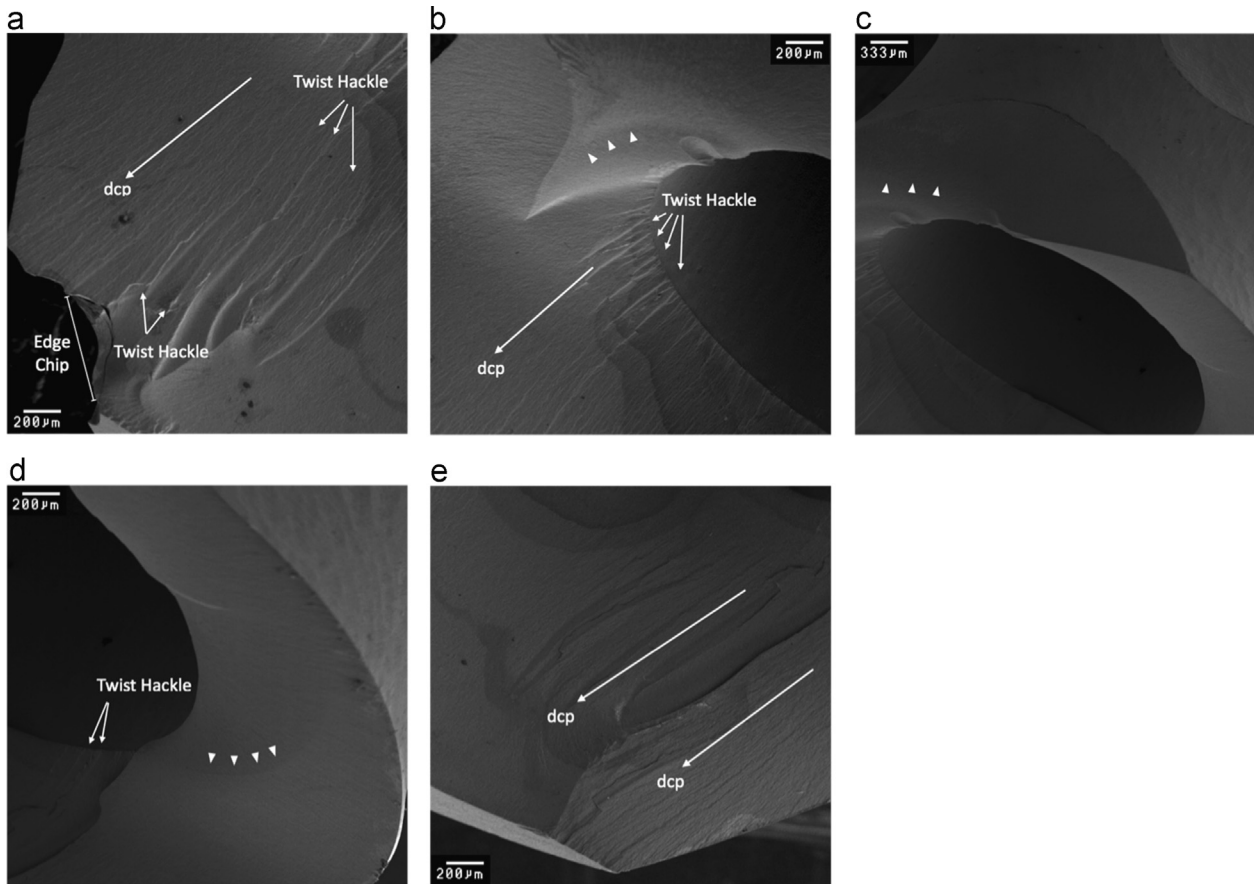


Fig. 5 – (a) SEM image of zone 1. Fractographic features like *twist hackle* and *micro-fine hackle lines* indicate that the crack was running downwards to the gingival margin. The big white arrow shows the dcp. However, it is possible to observe *twist hackle lines* departing from the edge chip on the gingival margin in the opposite direction. This edge chip crack is probably a secondary event related to the hexagon vertex as seen by the presence of many *hackle lines* propagating downwards. The white arrows propagating upwards indicate the *twist hackle* departing from the edge chip at the region related to hexagon vertex. **(b)** SEM image of zone 2 showing *twist hackle* emanating from the abutment region that was in contact with the lower edge of the abutment screw head and a lateral *arrest line* (white arrowheads). **(c)** SEM image of zone 3 showing the *compression curl* at the occlusal wall (white arrowheads). **(d)** SEM image of zone 4 showing fractographic features (*twist hackle*, lateral *arrest line* and *micro-fine hackle lines*) like the homologous zone. **(e)** SEM image of zone 5 showing fractographic features (*micro-fine hackle lines*) like the homologous zone.

Fig. 8a and b shows stereomicroscopic images of the metallic components. Some samples exhibited scratch marks on the screw head and fracture/deformation of the implant platform as indicated by the arrows.

4. Discussion

The fractographic analysis is a valuable tool to elucidate possible reasons for failure of ceramic pieces. The first important observation of this study was the differences in fracture patterns. Although damage modes in ceramic materials were studied in detail on flat surfaces, there have been few attempts of studying crack evolution, which demands a thorough investigation of the broken parts, in complex-geometries (Aboushelib et al., 2009; Aboushelib and Salameh, 2009; Belli et al., 2013; Lohbauer et al., 2010; Øilo et al., 2014; Quinn et al., 2005; Scherrer et al., 2008). In this

study, multiple cracks were sometimes propagated simultaneously in Y-TZP abutment-like complex geometries (see Fig. 1a). However, a general pattern of crack extension at the connecting area suggested that fracture started from this region.

Abutment fracture at the connecting area was also the main type of fracture found for Y-TZP abutments with external implant-abutment connection in many in vitro studies (Butz et al., 2005; Delben et al., 2014; Mühlemann et al., 2014; Truninger et al., 2012). In this regard, the discriminatory landmarks revealed by this fractographic approach made it possible to understand the reasons why this fracture pattern occurred. In screw-retained restorations, the screw access hole leads to a thinner abutment section (see Fig. 8a). Even with a high flexural strength (~ 900 MPa) and fracture toughness ($9 \text{ MPa m}^{1/2}$) (Rieger, 1989), thin sections seem to represent the weakest area of Y-TZP components (Aboushelib and Salameh, 2009; Passos et al., 2014). Indeed, tightening the

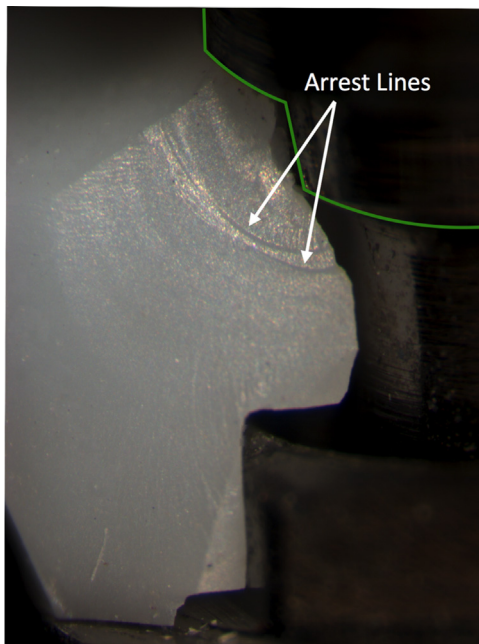


Fig. 6 – Stereomicroscopic image showing chip damage delimited by arrest lines (white arrows). The green line indicates the contour of the abutment screw head and highlights its proximity to the failure origin. (For interpretation of the references to color in this figure legend, the reader is referred to the web version of this article.)

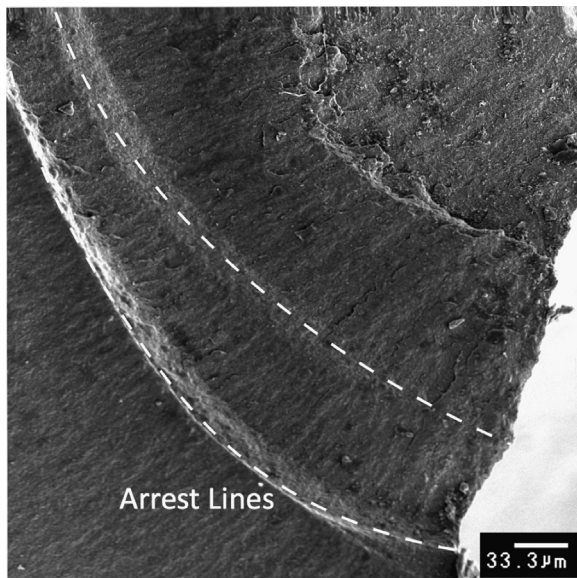


Fig. 7 – Higher magnification of Fig. 6, confirmed the presence of arrest lines (dashed white line) from which fine hackle lines emanated.

retention screw not only induces clamping forces that pull the prosthesis and implant together, but also generates high wedging forces inside the abutment (Aboushelib and Salameh, 2009). Classic fractographic features such as *arrest lines*, *hackle*, and *twist hackle* provided the general directions of

crack propagation. The failure-initiating defect clearly started where the Y-TZP abutment was in contact with the edges of the retention screw.

Although the secondary pattern near the loading point suggested that the fracture started from the contact point with the loading device, the SEM provided high magnification images, in which fine details such as the trails created by micro-fine *hackle* indicated that fracture propagated from the inner surface to the occlusal area (see Fig. 3d). In addition, frequent trails created by *hackle lines* moving outwards in all zones suggested tensile stress concentration on the inner surface of the abutment. The laboratory set-up may have been a source of tensile stresses. Upward loading on the lingual side of the abutment created a bending moment around the abutment screw head which acted as a fulcrum, causing tensile bending stresses to start from this region. It is interesting to note that the test procedures employed in this study (ISO 14801:2007) produced fractures that were comparable to the ones seen clinically (Aboushelib and Salameh, 2009; Passos et al., 2014) in which fracture started where the Y-TZP abutments were in contact with the internal metallic component (screw-nut). Thus, the test set-up was to some extent successful in simulating loading conditions in vivo.

It is also important to note that the screw head design has acute edges (see Figs. 4 and 5). This edge design is consistent with higher stress levels (Dundurs and Lee, 1972) and therefore unsuitable for Y-TZP abutments because of the characteristic brittleness of ceramic materials (Aboushelib and Salameh, 2009). In particular, it can be assumed that multiple implant-abutment connections in large Y-TZP infrastructures over implants may lead to more stress concentrations. The present findings indicated that the screw head and fitting surface of the abutment should have a rounded-edge design to ensure the integrity of Y-TZP implant restorations. Further studies using an in vitro set-up that achieve clinical fracture features as well as prospective long-term clinical studies should be conducted to elucidate the reasons why Y-TZP implant restorations fail. In addition, the damage of the external hex observed in some implants was also reported in previous studies as a result of the high hardness of Y-TZP abutments (Delben et al., 2014; Nguyen et al., 2009). Clinically, implant damage is a critical type of failure since it would probably require implant removal and repetition of the prosthetic work. Therefore, the mechanical behavior of such components should be better understood first to guarantee high reliability in the long term.

5. Conclusions

This study established a general pattern of crack extension at the connecting area and that the abutment screw designs could directly affect the occurrence of fractures in Y-TZP abutments. The present findings may also be used as reference for further fractographic analysis on retrieved Y-TZP implant restorations.

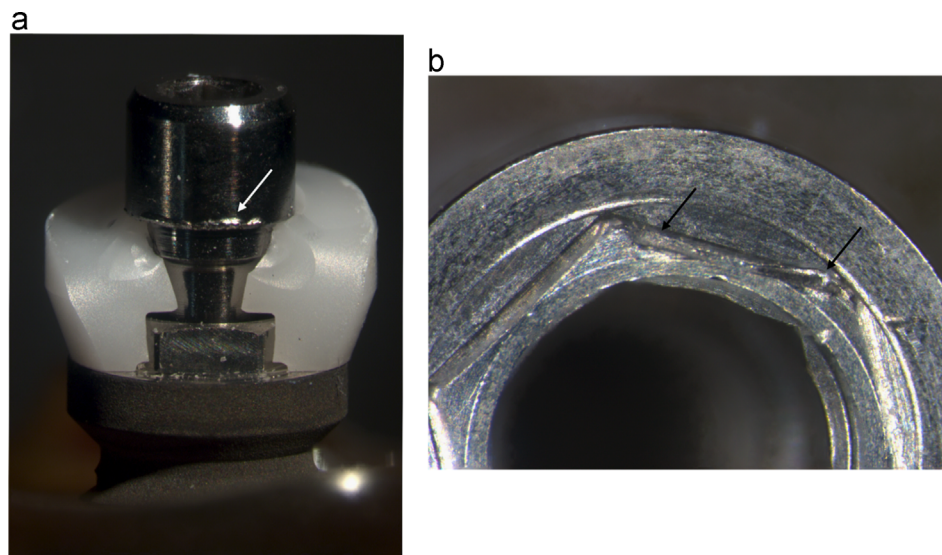


Fig. 8 – (a) Representative abutment screw damaged at the lower edge of the screw head (white arrow). (b) Representative implant damaged at the external hex platform (black arrows).

Acknowledgments

The authors gratefully acknowledge the assistance of Dr. Wirley Gonçalves Assunção for providing stereomicroscopy facilities and LME-IQ for providing SEM facilities. This work was partially supported by grant No. 2010/06651-5 from the São Paulo Research Foundation FAPESP.

REFERENCES

- Aboushelib, M.N., Salameh, Z., 2009. Zirconia implant abutment fracture: clinical case reports and precautions for use. *Int. J. Prosthodont.* 22, 616–619.
- Aboushelib, M.N., Feilzer, A.J., Kleverlaan, C.J., 2009. Bridging the gap between clinical failure and laboratory fracture strength tests using a fractographic approach. *Dent. Mater.* 25, 383–391.
- Belli, R., Petschelt, A., Lohbauer, U., 2013. Thermal-induced residual stresses affect the fractographic patterns of zirconia-veneer dental prostheses. *J. Mech. Behav. Biomed. Mater.* 21, 167–177.
- Butz, F., Heydecke, G., Okutan, M., Strub, J.R., 2005. Survival rate, fracture strength and failure mode of ceramic implant abutments after chewing simulation. *J. Oral Rehabil.* 32, 838–843.
- Delben, J.A., Barão, V.A., Ferreira, M.B., da Silva, N.R., Thompson, V.P., Assunção, W.G., 2014. Influence of abutment-to-fixture design on reliability and failure mode of all-ceramic crown systems. *Dent. Mater.* 30, 408–416.
- Dundurs, J., Lee, M.S., 1972. Stress concentration at a sharp edge in contact problems. *J. Elast.* 2, 109–112.
- Glauser, R., Sailer, I., Wohlwend, A., Studer, S., Schibli, M., Schärer, P., 2004. Experimental zirconia abutments for implant-supported single-tooth restorations in esthetically demanding regions: 4-year results of a prospective clinical study. *Int. J. Prosthodont.* 17, 285–290.
- ISO 14801:2007, 2007. Dentistry – Implants – Dynamic fatigue test for endosseous dental implants.
- Lohbauer, U., Amberger, G., Quinn, G.D., Scherrer, S.S., 2010. Fractographic analysis of a dental zirconia framework: a case study on design issues. *J. Mech. Behav. Biomed. Mater.* 3, 623–629.
- Lops, D., Bressan, E., Chiapasco, M., Rossi, A., Romeo, E., 2013. Zirconia and titanium implant abutments for single-tooth implant prostheses after 5 years of function in posterior regions. *Int. J. Oral Maxillofac. Implant* 28, 281–287.
- Mühlemann, S., Truninger, T.C., Stawarczyk, B., Hämmerle, C.H., Sailer, I., 2014. Bending moments of zirconia and titanium implant abutments supporting all-ceramic crowns after aging. *Clin. Oral Implant Res.* 25, 74–81.
- Nguyen, H.Q., Tan, K.B., Nicholls, J.I., 2009. Load fatigue performance of implant-ceramic abutment combinations. *Int. J. Oral Maxillofac. Implant* 24, 636–646.
- Øilo, M., Kvam, K., Tibballs, J.E., Gjerdet, N.R., 2013. Clinically relevant fracture testing of all-ceramic crowns. *Dent. Mater.* 29, 815–823.
- Øilo, M., Hardang, A.D., Ulsund, A.H., Gjerdet, N.R., 2014. Fractographic features of glass-ceramic and zirconia-based dental restorations fractured during clinical function. *Eur. J. Oral Sci.* 122, 238–244.
- Passos, S.P., Linke, B., Larjava, H., French, D., 2014. Performance of zirconia abutments for implant-supported single-tooth crowns in esthetic areas: a retrospective study up to 12-year follow-up. *Clin. Oral Implant Res.* 00, 1–8.
- Quinn, J.B., Quinn, G.D., Kelly, J.R., Scherrer, S.S., 2005. Fractographic analyses of three ceramic whole crown restoration failures. *Dent. Mater.* 21, 920–929.
- Rieger, W., 1989. *Medical Applications of Ceramics*. Academic Press, London.
- Scherrer, S.S., Quinn, G.D., Quinn, J.B., 2008. Fractographic failure analysis of a Procera Allceram crown using stereo and scanning electron microscopy. *Dent. Mater.* 24, 1107–1113.
- Truninger, T.C., Stawarczyk, B., Leutert, C.R., Sailer, T.R., Hämmerle, C.H., Sailer, I., 2012. Bending moments of zirconia and titanium abutments with internal and external implant-abutment connections after aging and chewing simulation. *Clin. Oral Implant Res.* 23, 12–18.
- Zembic, A., Sailer, I., Jung, R.E., Hämmerle, C.H., 2009. Randomized-controlled clinical trial of customized zirconia and titanium implant abutments for single-tooth implants in canine and posterior regions: 3-year results. *Clin. Oral Implant Res.* 20, 802–808.
- Zembic, A., Philipp, A.O., Hämmerle, C.H., Wohlwend, A., Sailer, I., 2015. Eleven-year follow-up of a prospective study of zirconia implant abutments supporting single all-ceramic crowns in anterior and premolar regions. *Clin. Implant Dent. Relat. Res.* 17, 2, <http://dx.doi.org/10.1111/cid.12263>.